Recent bright gully deposits on Mars: Wet or dry flow?

Jon D. Pelletier*
Department of Geosciences, University of Arizona, Tucson, Arizona 85721, USA
Kelly J. Kolb
Alfred S. McEwen
Department of Planetary Sciences, University of Arizona, Tucson, Arizona 85721, USA
Randy L. Kirk
United States Geological Survey, Astrogeology Program, 2255 N Gemini Drive, Flagstaff, Arizona 86001, USA

ABSTRACT

Bright gully sediments attributed to liquid water flow have been deposited on Mars within the past several years. To test the liquid water flow hypothesis, we constructed a high-resolution (1 m/pixel) photogrammetric digital elevation model of a crater in the Centauri Montes region, where a bright gully deposit formed between 2001 and 2005. We conducted one-dimensional (1-D) and 2-D numerical flow modeling to test whether the deposit morphology is most consistent with liquid water or dry granular flow. Liquid water flow models that incorporate freezing can match the runout distance of the flow for certain freezing rates but fail to reconstruct the distributary lobe morphology of the distal end of the deposit. Dry granular flow models can match both the observed runout distance and the distal morphology. Wet debris flows with high sediment concentrations are also consistent with the observed morphology because their rheologies are often similar to that of dry granular flows. As such, the presence of liquid water in this flow event cannot be ruled out, but the available evidence is consistent with dry landsliding.

Keywords: Mars, fluvial, mass wasting, numerical model.

INTRODUCTION

The bright gully sediments deposited on Mars within the past few years (Malin et al., 2006) have attracted great interest as possible signatures of liquid water flow under the present Martian climate. The distributary geometry of these deposits (Fig. 1A) resembles that of debris-fan deposits on Earth, suggesting that they were transported by a mixture of sediment and liquid water. This discovery, together with that of Amazonian-aged gullies morphologically consistent with fluvial erosion (Malin and Edgett, 2000; Gilmore and Phillips, 2002; Balme et al., 2006; Heldmann et al., 2007), has challenged the prevailing notion of a dry recent Mars. Alternatively, the recent gully deposits could be the result of dry mass wasting if source-region slopes are sufficiently steep. Granular materials can exhibit fluid-like behavior (Treiman, 2003; Shinbrot et al., 2004; Bart, 2007) and hence may produce depositional landforms very similar to those created by liquid water flow.

The bright color of the recent gully deposits was originally attributed to the presence of ice, frost, or salt residues (Malin et al., 2006). Given water-ice sublimation rates at bright gully deposit locations (Williams et al., 2007), the brightness can be expected to change significantly over time scales of at most 1–2 Martian years if the brightness is the result of ice or frost. Recent High Resolution Imaging Science Experiment (HiRISE) imagery, however, has observed no apparent change in deposit brightness since 2005, and Compact Reconnaissance Imaging Spectrometer (CRISM) spectra lack evidence of hydrated minerals such as salts (McEwen et al., 2007). However, brightly colored rocks in the Centauri Montes region outcrop in the source region above the bright gully deposit (Fig. 1A), suggesting that the deposit's bright color could be due to a distinctive source-rock lithology within either a wet or a dry flow. Alternatively, rock weathering on Mars could darken rock surfaces, causing clast breakup during transport to expose unweathered, brightly colored rock faces in the deposit. In addition, the deposit may be relatively fine grained, and would be brighter due to light scattering. These observations do not rule out a liquid water origin, but they do suggest that the bright color of recent deposits cannot be uniquely attributed to liquid water flow.

In addition to monitoring brightness changes through time, another means of distinguishing between wet and dry flow mechanisms is to determine which type of mechanism actually produces flow patterns most similar to those we observe. As a basis for this study, we mapped the topography in the part of the Centauri Montes region where the first bright gully deposit was discovered (Malin et al., 2006), by photogrammetric analysis of the stereo pair of HiRISE images PSP_001714_1415 and PSP_001846_1415. These images have scales of 0.25 m/pixel and a convergence angle of 22°. A digital elevation model (DEM) with a grid spacing of 1 m per post (Fig. 1A) was generated by using the area-based automatic image matching module of the commercial stereo software package SOCET SET (® BAE Systems) (Kirk et al., 2007). The estimated vertical precision of the DEM is 0.16 m, i.e., it contains spurious relief due to errors in matching the images with a root mean square (RMS) vertical amplitude of this order and horizontal dimensions of one to a few grid cells. The vertical precision of the DEM is sufficient to resolve the small-scale channels that convey the bright deposit flow, which range in depth from 0.3 to 1.5 m. The DEM was used as input to FLO-2D (FLO Engineering, 2006), a simulation code that solves the two-dimensional (2-D) dynamic wave momentum equation and volume conservation equation for the depth-averaged velocities at each time step using a Newton-Raphson iteration method. The code uses a Manning's roughness formulation to represent drag in the liquid water case and viscous and yield stresses to represent drag in the Bingham flow case. The Bingham flow capability of this software provides a basis for modeling dry granular flows in conjunction with 1-D kinematic modeling. The FLO-2D model is widely used in terrestrial applications for modeling unconfined water and debris flows in complex topographic environments.

*E-mail: jdpellet@email.arizona.edu.

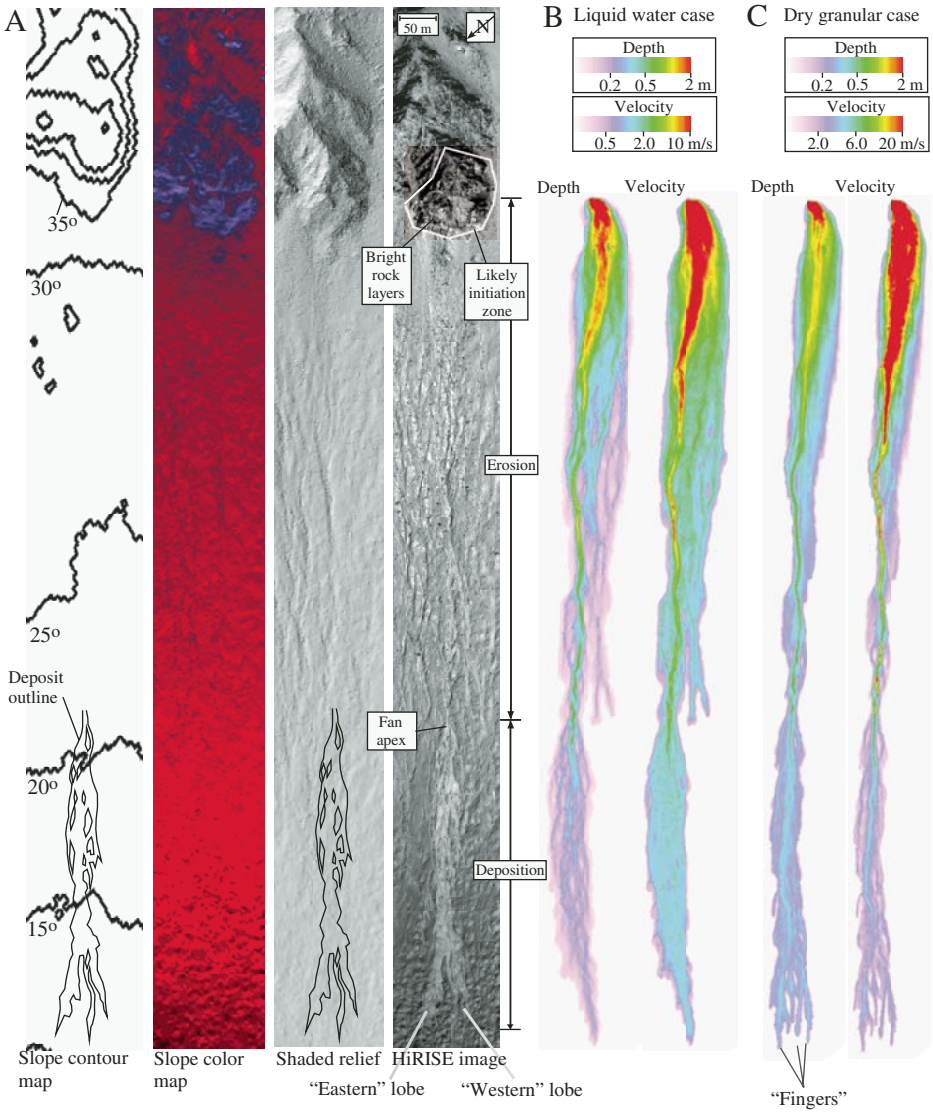

Figure 1. Two-dimensional model results and input data sets. A: Slope contour map, slope color map, shaded relief map, and portion of High Resolution Imaging Science Experiment (HiRISE) image (PSP_001714_1415) of initiation and runout zone of bright gully deposit in Centauri Montes region discovered by Malin et al. (2006) (see footnote 1). The slope map was spatially averaged before contouring to minimize microtopographic variability. B: Color maps of peak depth and velocity for the best-fit liquid water case with fluid-loss rate of 0.77 mm/s. C: Color maps of peak depth and velocity for dry granular case.

NUMERICAL MODELING

Pure Liquid Water Case

The initiation point of the bright gully deposit in the Centauri Montes region is not certain from the available images, but flow paths within the DEM suggest an initiation zone within a relatively small area near an outcrop of layered rocks (Fig. 1A). In addition, the HiRISE color image reveals a slight change in color of the materials below the rocky cliff (McEwen et al., 2007), consistent with recent disturbance. We began our liquid water simulation by releasing 2500 m^3 of water from a line source 10 m in length (perpendicular to flow direction) and 2 m in width over a period of 10 s at a location in the middle of the candidate initiation zone (Fig. 1A). Model results were not sensitive to the location or timing of the release (for a given volume), provided that the release rate was sufficiently high to produce critical flow in the release zone, thereby creating a flash flood. We used a spatially uniform Manning's n of 0.0545, and multiplied the roughness value by $\sqrt{g_E/g_M} = 1.62$, where g_E and g_M are the gravity constants for Earth and Mars (Wilson et al., 2004), before input into the FLO-2D model. The roughness value must be increased by the square root of the gravitational ratio because the acceleration of the flow is proportional to gravity but the drag term increases as the square root of gravity. To model the net effect of these two factors on fluid velocities requires that the effective drag coefficient n be increased by a factor of 1.62 in a model hard wired for Earth's gravity. Significant fluid loss during the time scale of the flood can occur by freezing in response to boiling and evaporative cooling (Heldmann et al., 2005) and, possibly, by infiltration. We treated these loss mechanisms collectively using a lumped parameter. The strength of the fluid-loss parameter controls the runout distance of the flow for a given release volume. As such, a best-fit fluid-loss rate can be determined by iteratively running the model with different loss rates for a fixed release volume until the model predicts a runout distance closest to observations. Treating the fluid-loss rate as a free parameter also implicitly incorporates the effects of soluble salts on freezing rates. This best-fit fluid-loss rate was determined to be 0.77 mm/s for this liquid water flow scenario. This value is ~7 times smaller than the Heldmann et al. (2005) estimate of 5.6 mm/s (i.e., 5.15 kg/m^2/s) based on 1-D thermohydraulic modeling for a hypothetical gully 0.3 m deep and 10 m wide assuming pure water and no infiltration. If we adopt the Heldmann et al. (2005) value, the release volume must be increased by a factor of ~7 to match the runout distance for this event. However, such a large-release scenario causes widespread, unconfined flooding (even if the initiation point is moved downslope and the fluid-loss rate is increased up to 1.5 mm/s) that is not consistent with the observed pattern of flow based on where bright sediment deposition actually occurred.

Model results (Fig. 1B; see also animation in GSA Data Repository Appendix DR1[1]) predict that a liquid water flow event will run out to a total horizontal distance of 1.25 km from the initiation point in a period of 7 min with maximum flow depths of 1.0 m (not including the proximal flow region) and peak velocities of ~8 m/s (Fig. 1B) for this model scenario. In the distal flow region of the actual event, bright sediment deposition provides a map of where flow occurred (Fig. 1A). Inundated areas predicted by the model are generally in good agreement with observations. However, the distal lobe morphology predicted by the model is not in good agreement with the observed lobe morphology. In the actual deposit, both a western and an eastern lobe are formed. In the liquid water model, all of the flow is routed to the western lobe, the bed

[1]GSA Data Repository item 2008055, animations of liquid water and dry granular flow models for bright gully deposit in Centauri Montes, Mars, and a spreadsheet that implements the 1-D dry granular flow model, is available online at www.geosociety.org/pubs/ft2008.htm, or on request from editing@geosociety.org or Documents Secretary, GSA, P.O. Box 9140, Boulder, CO 80301, USA.

of which is topographically lower than the bed beneath the eastern lobe. Given the shallow flow depths (i.e., 0–30 cm) in this distal flow region, it is not surprising that bed topography plays the dominant role in controlling the flow pathway.

Dry Granular Flow Case

Dense, dry granular flows can be modeled within a kinematic or fluid-dynamic framework. In the kinematic framework, the friction coefficient of a dense granular flow on a rough surface (Jop et al., 2006) is given by

$$\mu(I) = \tan\theta_s + \frac{\tan\theta_2 - \tan\theta_s}{I_0/I + 1}, \qquad (1)$$

where μ is the friction coefficient, $\tan\theta_s$ and $\tan\theta_2$ are minimum and maximum kinetic friction coefficients, I_0 is an experimentally determined constant equal to 0.279, and I is a dimensionless number equal to $\dot{\gamma}d/\sqrt{P/\rho_s}$, where $\dot{\gamma}$ is the shear rate, d is the mean grain diameter, P is the compressive stress, and ρ_s is the density of the solid material. The values of θ_s and θ_2 are nominally 21° and 33° for smooth, sand-sized particles, but vary according to grain size and surface roughness (e.g., experiments with a range of particle sizes from medium to coarse sand yield θ_s = 20.7°–22.9°; Pouliquen, 1999). Physically, θ_2 is the angle of repose and θ_s is the angle below which active flows begin to decelerate on the slope. The compressive stress at the base of the flow is equal to $\rho_b gh$, where ρ_b is the bulk density of the flow, g is gravity, and h is the thickness. Equation 1 has been verified experimentally in variable-gravity experiments (Baran and Kondic, 2006) (i.e., θ_s and θ_2 are material properties; the effects of variable gravity are captured entirely in I). For a flow of thickness h and depth-averaged velocity v, the shear rate is equal to $2v/h$, giving $I = 2vd\sqrt{\rho_b g/\rho_s h}$. Equation 1 reduces to a Bingham (viscoplastic) rheology in the fluid-dynamic framework, with a velocity-dependent viscosity and yield stress (Jop et al., 2006) given by

$$\eta = \mu(I)P/\dot{\gamma} \text{ and } \tau_y = \mu(I)P. \qquad (2)$$

In equation 2, the viscosity goes to infinity as the shear rate (or velocity) goes to zero. This leads to the rapid "jamming" of granular flows as they slow down near the base of a slope.

We constructed a 1-D kinematic model of dry granular flows on Mars to complement the 2-D fluid-dynamic model and to estimate the Bingham model parameters needed as input for the 2-D model. The 1-D model (implemented in MS Excel; see the Data Repository) solves Newton's law of motion for a dry granular flow of constant thickness moving down a variably inclined slope (Fig. 2A) with friction coefficient given by Equation 1. Model results (Fig. 2B) indicate that a dry granular flow initiated from the same location as the 2-D model will run out a distance of 1.1–1.4 km horizontally from the initiation point, with longer distances corresponding to thicker and/or finer grained flows. The median grain size of the actual flow is unknown, but it is likely within the range of fine to coarse sand we considered (Fig. 2B). The 1-D model predicts an event of 1.5 min duration with peak velocities of ~20 m/s. Post-processing of the velocity profiles indicates that the effective yield stress for a sand-dominated material with a thickness of 0.5 m is ~1000 Pa. The viscosity is inversely proportional to the instantaneous velocity, but has event-averaged values of 50–100 Pa s (Fig. 2C).

Currently, the FLO-2D model does not incorporate a velocity-dependent viscosity, so the 2-D dry granular flow model implemented in FLO-2D uses a constant viscosity given by the average viscosity calculated from the 1-D model (which includes velocity-dependent friction and viscosity) for a given event. The validity of this constant-viscosity assumption for the 2-D case is supported by the fact that the viscosities calculated from the 1-D model vary by <20% from the average value over ~80% of the flow distance (i.e., the viscosity in Fig. 2C is relatively constant except for the very beginning and end of the flow, where viscosity is much larger due to the much lower velocity and shear rate). In order to represent Mars' gravity in the FLO-2D model for the dry granular flow case, we multiplied the yield stress by the gravitational ratio g_E/g_M = 2.63 before input into FLO-2D. This linear scaling is necessary because the thickness of a plastic flow is inversely proportional to gravity for a constant yield stress, so to correct for Mars' lower gravity we need to multiply the yield stress by 2.63 to predict the correct flow thickness within a model hard wired for Earth's gravity. The viscosity value needs no correction because the acceleration and viscous drag terms are both proportional to gravity, and so these effects cancel out when predicting flow velocities in the dry granular case.

Here we report 2-D model results with τ_y = 1000 Pa and η = 50 Pa s (corresponding to a sand-textured flow with an average thickness of 0.5 m) (Fig. 2C; see also animation in Appendix DR1). Identical initial conditions were used as in the pure liquid water case except that the fluid was released in 2 s instead of 10 s over an area of 100 m² instead of 20 m² (i.e., faster initiation is appropriate for a rock-fall–initiation scenario). The model predicts flow geometries very similar to observations, especially near the distal end of the deposit where the model forms two primary depositional lobes (and several smaller, secondary lobes) similar in shape to the western and eastern lobes of the actual deposit. Lobe fingering in simulations of the dry granular case was a robust feature; i.e., only by increasing the yield stress to unrealistically high values could we disable this fingering behavior. The distributary pattern of the fingers is not sensitive to bed topography (i.e., flow occurs in both lobes despite the lower topographic position of the western channel). This is consistent with the thicker, more viscous nature of dry granular flow compared to liquid water flow. Overall, the dry granular flow case is characterized by a more uniform cross-sectional velocity profile compared to that of liquid water flow case, which is consistent with the "plug" nature of viscoplastic flows. The model results, including the runout distance of the flow, depend on user-defined choices for the release volume, median grain size, and flow initiation point. Overall, however, we were struck by the similarity of the model predictions with the observed pattern of bright sediment deposition for a wide range

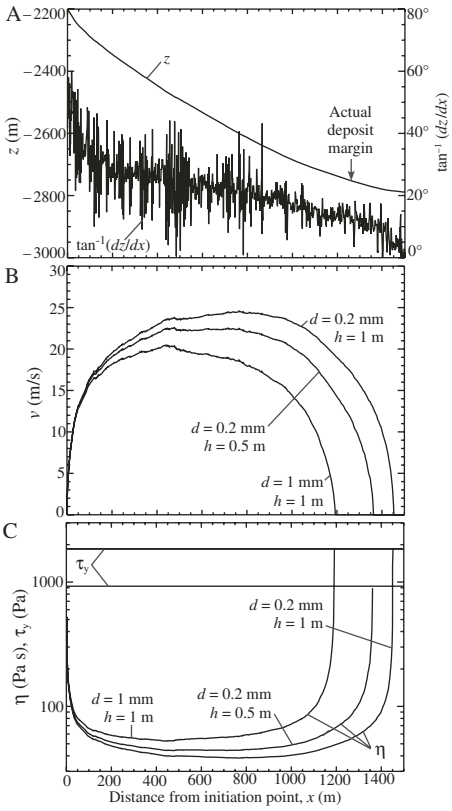

Figure 2. One-dimensional kinematic model results for dry granular flow. A: Along-channel elevation and slope angle of bright gully deposit (data extracted from photogrammetric digital elevation model), as function of distance from initiation point, with deposit margin indicated. B: Model predictions for velocity of the granular flow as function of distance for three different combinations of flow thickness and median grain size. Thicker and finer-grained flows have longer runout distances. C: Yield stress τ_y and dynamic viscosity η corresponding to the model examples in B, according to equation 2.

of reasonable initial conditions and grain sizes. Although we assumed a localized source for this event, it is likely that the source was spatially distributed, i.e., that a small rock fall triggered landsliding downslope, causing the flow to bulk up gradually within the proximal source region. Model results with a more distributed source yield similar flow patterns and runout distances to those of the localized source case.

DISCUSSION

The overall pattern of erosion and deposition observed in this flow event (erosion upstream of the fan apex, deposition downstream of the apex) is consistent with the mechanics of a dry granular flow. The steepest colluvial slopes downslope from the initiation point are close to the 33° angle of repose (Fig. 1A). The transition from erosion to deposition occurs where the slope angle is 21° ±0.5° (microtopographic variability limits the precision of local slope values) (Fig. 1A). This angle coincides with the transition from accelerating flow to decelerating flow in the 1-D model, and so where the transition from erosion to deposition should be expected. The kinetic friction angle θ_s in equation 1 plays an important role in the mechanics of dry granular flows. Evaluations of dry mass-wasting hypotheses on Mars often consider only the static friction angle and, if average slopes are lower than that angle, conclude that dry granular flow cannot be responsible for the observed flow (Heldmann et al., 2007). Granular flows, however, can accelerate and erode at any angle above θ_s, as long as they achieve sufficient momentum from steeper portions of the source region before the slope angle drops below θ_2. Dry granular flows initiated from steep slopes can, therefore, be divided into three kinematic zones. In areas where the topographic slope angle $\tan^{-1}(dz/dx)$ is $>\theta_2$, the flow undergoes acceleration. In areas where $\theta_s < \tan^{-1}(dz/dx) < \theta_2$, static granules remain stationary, but fast flows triggered from steep upslope source regions continue to accelerate. In areas where $\tan^{-1}(dz/dx) < \theta_s$, all flows decelerate regardless of flow velocity. This framework suggests that dry granular sediments should be deposited on slopes at or <21° when they originate from steep source regions. More broadly, both friction angles should be considered when evaluating dry mass-wasting hypotheses on Mars.

Wet debris flows on Earth with relatively high (i.e., 0.4–0.5) volumetric sediment concentrations typically have viscosities and yield stresses on the order of 100 Pa s and 1000 Pa, respectively (O'Brien and Julien, 1988). As such, wet debris flows can be expected to produce flow patterns similar to that of the dry granular flow case considered here. Given the order-of-magnitude variability in the viscosities and yield stresses of sediment-rich debris flows on Earth, it would be difficult for a modeling study to distinguish between dry granular flow and wet debris flow given current data. This conclusion also applies to other debris flows on Mars, where previous modeling has shown that Bingham flow models with viscosities and yield stresses of the same order as those used here are consistent with observed morphologies (Mangold et al., 2003; Miyamoto et al., 2004). We cannot, therefore, rule out the presence of liquid water in this flow event. Our results clearly illustrate, however, that liquid water is not required to form this particular deposit in the Centauri Montes region. Given the difficulty of producing or delivering water to the surface of Mars in the current climate (Mellon and Phillips, 2001), the dry flow model must be considered more likely. More broadly, our modeling approach provides a useful framework for testing wet versus dry flow hypotheses for other slope deposits and for understanding potential links between dry mass-wasting processes and longer-term landform evolution on Mars.

ACKNOWLEDGMENTS

Pelletier acknowledges funding by the National Aeronautics and Space Administration Mars Fundamental Research Program, grant NNG05GM30G. Kolb, McEwen, and Kirk acknowledge funding from the High Resolution Imaging Science Experiment (HiRISE), Jet Propulsion Laboratory contract 1272218. We thank Elpitha Howington-Kraus for implementing the software needed to work with HiRISE images on our photogrammetric workstation, and for producing the digital terrain model used in this project. We also thank Alan Treiman, Hirdy Miyamoto, and an anonymous reviewer for helpful comments that improved the manuscript.

REFERENCES CITED

Balme, M., Mangold, N., Baratoux, D., Costard, F., Gosselin, M., Masson, P., Pinet, P., and Neukum, G., 2006, Orientation and distribution of recent gullies in the southern hemisphere of Mars: Observations from High Resolution Stereo Camera/Mars Express (HRSC/MEX) and Mars Orbiter Camera/Mars Global Surveyor (MOC/MGS) data: Journal of Geophysical Research, v. 111, doi: 10.1029/2005JE002607.

Baran, O., and Kondic, L., 2006, On velocity profiles and stresses in sheared and vibrated granular systems under variable gravity: Physics of Fluids, v. 18, 121509, 9 p.

Bart, G.D., 2007, Comparison of small lunar landslides and martian gullies: Icarus, v. 187, p. 417–421, doi: 10.1016/j.icarus.2006.11.004.

FLO Engineering Inc, 2006, FLO-2D user manual, version 2006.1: Nutrioso, Arizona, FLO Engineering Inc.

Gilmore, M.S., and Phillips, E.L., 2002, Role of aquicludes in formation of Martian gullies: Geology, v. 30, p. 1107–1110, doi: 10.1130/0091–7613(2002)030<1107:ROAIFO>2.0.CO;2.

Heldmann, J.L., Toon, O.B., Pollard, W.H., Mellon, M.T., Pitlick, J., McKay, C.P., and Andersen, D.T., 2005, Formation of martian gullies by the action of liquid water flowing under current martian environmental conditions: Journal of Geophysical Research, v. 110, doi: 10.1029/2004JE002261.

Heldmann, J.L., Carlsson, E., Johansson, H., Mellon, M.T., and Toon, O.B., 2007, Observations of martian gullies and constraints on potential formation mechanisms. II. The northern hemisphere: Icarus, v. 188, p. 324–344, doi: 10.1016/j.icarus.2006.12.010.

Jop, P., Forterre, Y., and Pouliquen, O., 2006, A constitutive law for dense granular flows: Nature, v. 441, p. 727–730, doi: 10.1038/nature04801.

Kirk, R.L., Howington-Kraus, E., Rosiek, M.R., Cook, D., Anderson, J., Becker, K., Archinal, B.A., Kesthelyi, L., King, R., and McEwen, A.S., 2007, Ultrahigh resolution topographic mapping of Mars with HiRISE stereo images: Methods and first results: Proceedings of the 7th International Conference on Mars: Houston, Texas, Lunar and Planetary Institute, http://www.lpi.usra.edu/meetings/7thmars2007/pdf/3381.pdf.

Malin, M.C., and Edgett, K.S., 2000, Evidence for recent groundwater seepage and surface runoff on Mars: Science, v. 288, p. 2330–2335, doi: 10.1126/science.288.5475.2330.

Malin, M.C., Edgett, K.S., Posiolova, L.V., McCauley, S.M., and Noe Dobrea, E.Z., 2006, Present-day impact cratering rate and contemporary gully activity on Mars: Science, v. 314, p. 1573–1577, doi: 10.1126/science.1135156.

Mangold, N.F., Costard, F., and Forget, F., 2003, Debris flows over sand dunes on Mars: Evidence for liquid water: Journal of Geophysical Research, v. 108, doi: 10.1029/2002JE001958.

McEwen, A.S., and 31 others, 2007, HiRISE observations of recent water-related geologic activity on Mars: Science, v. 317, p. 1706–1709.

Mellon, M.T., and Phillips, R.J., 2001, Recent gullies and the source of liquid water: Journal of Geophysical Research, v. 106, p. 23,165–23,180, doi: 10.1029/2000JE001424.

Miyamoto, H., Dohm, J.M., Baker, V.R., Beyer, R.A., and Bourke, M., 2004, Dynamics of unusual debris flows on Martian sand dunes: Geophysical Research Letters, v. 31, doi: 10.1029/2004GL020313.

O'Brien, J.S., and Julien, P.Y., 1988, Laboratory analysis of mudflow properties: Journal of Hydraulic Engineering, v. 114, p. 877–887.

Pouliquen, O., 1999, Scaling laws in granular flows down rough inclined planes: Physics of Fluids, v. 11, p. 542–548, doi: 10.1063/1.869928.

Shinbrot, T., Duong, N.H., Kwan, L., and Alvarez, M.M., 2004, Dry granular flows can resemble some Martian geological features attributed to liquid flow: National Academy of Sciences Proceedings, v. 101, p. 8542–8546, doi: 10.1073/pnas.0308251101.

Treiman, A.H., 2003, Geologic setting of the Martian gullies: Implications for their origins: Journal of Geophysical Research, v. 108, doi: 10.1029/2002JE001900.

Williams, K.E., Toon, O.B., and Heldmann, J., 2007, Modeling water ice lifetimes at recent Mars gully locations: Geophysical Research Letters, v. 34, doi: 10.1029/2007GL029507.

Wilson, L., Ghatan, G.J., Head, J.W., and Mitchell, K.L., 2004, Outflow channels: A reappraisal of the estimation of water flow velocities from water depths, regional slopes, and channel floor properties: Journal of Geophysical Research, v. 109, doi: 10.1029/2004JE002281.

Manuscript received 7 August 2007
Revised manuscript received 2 November 2007
Manuscript accepted 6 November 2007

Printed in USA